4146–4152 *Nucleic Acids Research, 1998, Vol. 26, No. 18*

Mapping of interaction domains between human repair proteins ERCC1 and XPF

Wouter L. de Laat, Anneke M. Sijbers, Hanny Odijk, Nicolaas G. J. Jaspers and Jan H. J. Hoeijmakers*

Department of Cell Biology and Genetics, Medical Genetics Centre, Erasmus University, PO Box 1738, 3000 DR Rotterdam, The Netherlands

Received June 11, 1998; Revised and Accepted July 24, 1998

ABSTRACT

ERCC1–XPF is a heterodimeric protein complex involved in nucleotide excision repair and recombinational processes. Like its homologous complex in *Saccharomyces cerevisiae*, Rad10–Rad1, it acts as a structure-specific DNA endonuclease, cleaving at duplex–single-stranded DNA junctions. In repair, ERCC1–XPF and Rad10–Rad1 make an incision on the the 5′-side of the lesion. No humans with a defect in the ERCC1 subunit of this protein complex have been identified and ERCC1-deficient mice suffer from severe developmental problems and signs of premature aging on top of a repair-deficient phenotype. Xeroderma pigmentosum group F patients carry mutations in the XPF subunit and generally show the clinical symptoms of mild DNA repair deficiency. All XP-F patients examined demonstrate reduced levels of XPF and ERCC1 protein, suggesting that proper complex formation is required for stability of the two proteins. To better understand the molecular and clinical consequences of mutations in the ERCC1–XPF complex, we decided to map the interaction domains between the two subunits. The XPF-binding domain comprises C-terminal residues 224–297 of ERCC1. Intriguingly, this domain resides outside the region of homology with its yeast Rad10 counterpart. The ERCC1-binding domain in XPF maps to C-terminal residues 814–905. ERCC1–XPF complex formation is established by a direct interaction between these two binding domains. A mutation from an XP-F patient that alters the ERCC1-binding domain in XPF indeed affects complex formation with ERCC1.

INTRODUCTION

Nucleotide excision repair (NER) is a cellular process that guards the integrity of the genome. It removes a wide variety of lesions from the DNA, including bulky DNA adducts and the most prominent UV-induced damages. During NER, a dual incision is made asymmetrically around a lesion to allow its release as part of a larger (24–32 nt) DNA fragment (1–3). The remaining gap is filled by DNA synthesis and ligation (4; comprehensively reviewed in 5). The mammalian heterodimeric protein complex ERCC1–XPF is a structure-specific endonuclease that catalyzes incision on the 5′-side of the lesion during NER (6–8). Like XPG, which makes the 3′ incision (9), ERCC1–XPF is thought to be positioned through protein–protein interactions with other repair factors around a partially unwound DNA intermediate (10–12). Defects in one of the XP factors (XPA-G) involved in the incision stage of NER can cause the typical UV-sensitive, cancer-prone phenotype observed with xeroderma pigmentosum patients.

Chinese hamster cell lines defective in either ERCC1 or XPF show not only sensitivity to UV light, but are also extremely sensitive to DNA interstrand cross-linking agents, a phenomenon not observed with any other NER-deficient cell line (13). Mutational analysis of the *ERCC1* gene *in vivo* showed that indeed most mutations affecting its NER function also disrupt its presumed function in the repair of interstrand cross-links (14). Moreover, severe symptoms like liver and kidney abnormalities, developmental delay, reduced lifespan and signs of premature senescence are typically observed with ERCC1 knock-out mice and are absent in NER-deficient XPA and XPC knock-out mice (15–19). In *Saccharomyces cerevisiae*, strains defective in the homologs of ERCC1 and XPF, Rad10 and Rad1, fail to complete recombination between direct repeated DNA sequences (20) and mutations in the homologous proteins of *Schizosaccharomyces pombe*, Swi10 and Rad16, can affect mating-type switching (21). An additional engagement of ERCC1–XPF and their homologs in recombinational pathways might commonly underlie these non-NER-related phenotypes.

There is limited knowledge of structural and functional domains within the ERCC1–XPF complex. Protein–protein interactions have been reported with the putative damage recognition protein XPA (22–24) and with the single-stranded DNA-binding protein RPA (replication protein A) (25,26), which may stabilize the opened DNA complex (11,12). The interaction with XPA occurs through residues 93–120 in the ERCC1 protein (22). Recently, we demonstrated that RPA can modulate ERCC1–XPF incision activity such that cleavage is restricted to the damaged strand (W.L.de Laat *et al*., submitted for publication). It is as yet unknown which region in ERCC1–XPF is responsible for the interaction with RPA. At the C-terminus of the ERCC1 protein, a region of 53 residues shows extensive homology to the

*To whom correspondence should be addressed. Tel: +31 10 4087199; Fax: +31 10 4360225; Email: hoeijmakers@gen.fgg.eur.n

C-terminus of the *Escherichia coli* NER protein UvrC (27,28). In UvrC, this region was found to be essential for its endonuclease activity (29) and deletion of this region specifically disrupted the 5′ incision during NER in *E.coli* (30). Possibly, these residues are required to position the active cleavage site correctly onto the DNA (30). In agreement, the region comprises a so-called helix–hairpin–helix (HhH) motif, which has been implicated in non-sequence-specific DNA binding and was found to be present in many DNA break processing enzymes (14,31), including the structure-specific DNA nucleases FEN-1 and XPG (32,33). The 20 amino acid long HhH motif, present twice in this C-terminal part of ERCC1, is the only domain that ERCC1–XPF shares with other structure-specific nucleases. Intriguingly, the *S.cerevisiae* Rad1–Rad10 complex lacks this UvrC-like domain, including the HhH motifs, but incises DNA at exactly the same positions as ERCC1–XPF (8).

A more detailed map of functional domains within the ERCC1 and XPF proteins might provide insight into the relevance of sequence motifs within this complex. Also, it would allow a more accurate interpretation of the phenotypical consequences of mutations in the encoding genes. Here we report the mapping of the interaction domains between ERCC1 and XPF and we demonstrate directly that a naturally occurring XPF mutation affects complex formation.

MATERIALS AND METHODS

Construction of mutant cDNAs

N-Terminal truncations were made via PCR using sense primers containing (5′→3′) a T7 polymerase recognition sequence, an optimal translational initiation sequence and 18–24 nt complementary to the sequence of insertion. Exceptions were the constructs XPF-ATG629, XPF-ATG677, XPF-ATG711 and XPF-ATG737. Here, the restriction sites *Hin*dIII, *Rsa*I, *Fok*I and *Eag*I were used, respectively, to remove upstream coding cDNA in front of these in-frame ATG codons. HA epitope tags were introduced as described previously (6). C-Terminal truncations were made via PCR using antisense primers containing (3′→5′) 18–24 complementary nucleotides, a translational stop sequence and 6–9 random nucleotides. cDNA from the two alleles of XP126LO was amplified, subcloned and sequenced as described (8).

In vitro translations and immunoprecipitations

ERCC1 and XPF constructs were transcribed and translated separately *in vitro*, following the instruction manual of the TnT coupled transcription-translation system of Promega. PCR products were phenol extracted and ethanol precipitated; 2–10 µg DNA were added per 50 µl *in vitro* transcription/translation reaction mix. The polyclonal antibodies against ERCC1 and XPF (affinity-purified) used for immunoprecipitations have been described before (8,34). For immunoprecipitations, (truncated) ERCC1 protein and (truncated) XPF protein were mixed with 5 µl NETT buffer (100 nM NaCl, 5 mM EDTA, 50 mM Tris, pH 7.5, and 0.5% Triton X-100) (total volume 15–20 µl) and incubated for 30 min at 30°C. Antibody was added and after 2 h at 4°C, 100 µl NETT buffer containing 10% protein A–Sepharose beads were added. Incubation proceeded for another 2 h at 4°C (with tumbling), then the beads were washed four times with 0.5 ml NETT and suspended in sample buffer. Samples were boiled and protein fragments were separated on SDS–polyacrylamide gels, which varied between 5 and 16.5% acrylamide, depending on the size of the peptides studied. In the case of 15 and 16.5% gels, 0.1 M NaAc was added to the lower running buffer for optimal separation of small protein fragments and the dye *m*-cresol purple was added to sample buffer, instead of Coomassie blue (35). Dried gels were analyzed by autoradiography or with a phosphorimager.

RESULTS

ERCC1 and XPF efficiently reconstitute a protein complex *in vitro*

In mammalian cells, endogenous ERCC1 and XPF are associated in a stable heterodimeric protein complex (8,23,34,36) and complex formation *in vivo* was also observed when recombinant ERCC1 and XPF proteins were overproduced together in insect cells (6,25) or *E.coli* (unpublished observation). To determine whether ERCC1 and XPF associate *in vitro*, immunoprecipitations were performed on *in vitro* translated gene products. For this purpose, affinity-purified polyclonal antibodies against ERCC1 and XPF were used that had previously been shown to be able to deplete the complex from whole cell extracts (8,34). *In vitro* translation of XPF in a reticulocyte lysate-based transcription/translation system resulted not only in the 115 kDa full-length gene product but also in a series of truncated polypeptides which could be precipitated with an anti-XPF antibody (Fig. 1, lane 4). Consistent with their molecular weight, these fragments appeared to originate from in-frame alternative start codons. When XPF protein was incubated with anti-ERCC1 antibodies alone, no significant XPF precipitation was observed, showing minimal cross-reactivity with the anti-ERCC1 antibody (Fig. 1, lane 2). However, addition of *in vitro* translated ERCC1 (Fig. 1, lane 1) resulted in efficient XPF precipitation with anti-ERCC1 antibodies (Fig. 1, lane 3), demonstrating complex formation between ERCC1 and XPF. Similarly, precipitation of wild-type ERCC1 with anti-XPF antibodies was detected only in the presence of XPF protein (Fig. 1, compare lanes 5 and 6). In all these tests, the corresponding pre-immune antiserum and an unrelated antiserum raised against XPA protein were not able to precipitate any complex; patterns were not different from the beads-only controls in Figure 1, lanes 2 and 5 (data not shown). We conclude that ERCC1 and XPF efficiently reconstitute a protein complex *in vitro*. As this assay detects binding of small amounts of proteins amidst a vast excess of reticulocyte lysate-derived proteins, it has to be considered a stringent binding assay, detecting high affinity interactions only. As such, it will provide a conservative estimate of the domains responsible for complex formation.

The XPF-binding domain is localized to the C-terminal region of ERCC1

Localized protein–protein interaction domains were previously assigned in Rad1–Rad10, the homologous counterpart of the ERCC1–XPF complex in *S.cerevisiae* (37,38). Almost two thirds of the Rad10 protein, stretching from residue 90 to 210 at the very C-terminus, was shown to be required for Rad1 binding. This region corresponds to amino acids 98–214 in ERCC1, i.e. the middle part of this protein. In order to identify the XPF-binding domain in ERCC1, initial truncations from both sides of the ERCC1 protein were based on this putative interaction domain.

The first 92 amino acids at the N-terminus of ERCC1 were found to be dispensable for XPF binding and, in contrast to

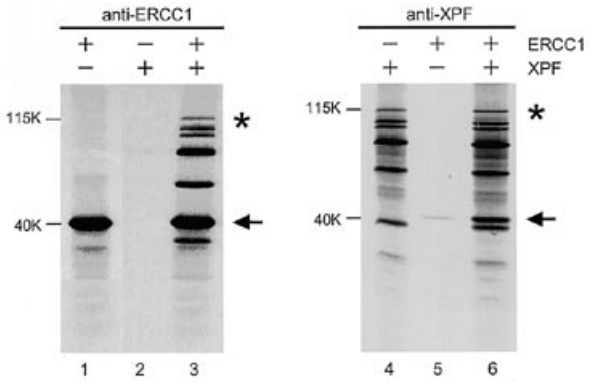

Figure 1. *In vitro* translated ERCC1 and XPF reconstitute a complex. Autoradiogram of (antibody bead-bound) ^{35}S-labeled proteins separated on an 11% SDS–polyacrylamide gel. Input is indicated above each lane. ERCC1 and XPF *in vitro* translates directly analyzed on the gel show identical products, as observed in lanes 1 and 4, respectively. An asterisk indicates full-length XPF protein, an arrow indicates full-length ERCC1 protein. The molecular weights of the full-length proteins are indicated.

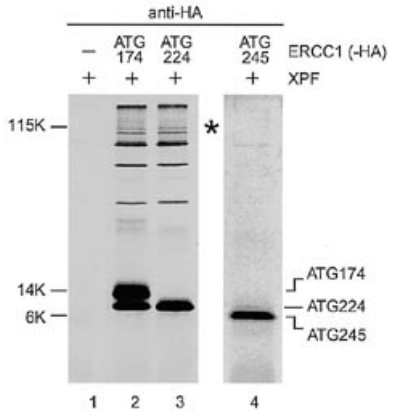

Figure 2. N-Terminal truncations of ERCC1. Autoradiogram of (antibody bead-bound) ^{35}S-labeled proteins separated on a 16.5% SDS–polyacrylamide gel. Note that only the ERCC1 protein fragments carry an HA epitope tag. The lower band synthesized along with ERCC1-ATG174 (lane 2) originates from the in-frame alternative translational start at position 224 in ERCC1 and also carries an HA epitope tag at the C-terminus. Production and visualization of the very small (6 kDa) ERCC1-ATG245 fragment was difficult; co-precipitation of XPF with this fragment was performed in a separate experiment and is shown as a distinct panel (lane 4). The altered migration pattern of *XPF* gene products (compared with Fig. 1) is due to a different percentage of gel. An asterisk indicates full-length XPF protein. The molecular weights of the proteins are indicated.

Rad10, deleting the N-terminal 103 residues (ERCC1-ATG103) and 118 residues (ERCC1-ATG118) did not seem to affect complex formation either. Even subsequent truncations from the N-terminus did not abolish the XPF binding capacity of ERCC1 and, much to our suprise, we found that an ERCC1 peptide lacking the complete region of homology to Rad10 (ERCC1-ATG224) still bound to XPF (Fig. 2, lanes 2 and 3). This interaction was observed with both an anti-XPF antibody (data not shown) and with an antibody directed against an HA epitope tag introduced at the C-terminus of the ERCC1 fragments (Fig. 2). The latter had to be used because the anti-ERCC1 antibody failed to precipitate such small C-terminal ERCC1 peptides. Deleting the N-terminal 245 residues of ERCC1, yielding a peptide with a molecular weight of only 6 kDa, abolished the affinity for XPF (Fig. 2, lane 4). We conclude that the N-terminal border of the domain responsible for initial and stable binding to XPF resides between residues 224 and 245 in the ERCC1 protein (Fig. 4).

In agreement with this conclusion, a C-terminally truncated ERCC1 protein containing only the first 215 residues (ERCC1-STOP215) was deficient in XPF binding. The same was found for the proteins ERCC1-STOP235, ERCC1-STOP257 (data not shown) and ERCC1-STOP282 (Fig. 3, lanes 7 and 8). Even ERCC1-STOP292, lacking only five amino acids from the C-terminus of full-length ERCC1, did not show XPF binding (Fig. 3, lanes 5 and 6). Interestingly, the addition of residue Phe293 to ERCC1-STOP292, yielding ERCC1-STOP293, reproducibly restored partial affinity for XPF, possibly demonstrating a direct involvement of this phenylalanine in XPF binding (Fig. 3, lanes 3 and 4). However, ERCC1-STOP293 never co-precipitated with XPF as efficiently as did full-length ERCC1, showing that even the last four residues contained sequence information required for optimal XPF binding. We conclude therefore that the C-terminal border of the XPF-binding domain in ERCC1 is located between residues 293 and 297, which is the last amino acid of full-length ERCC1 (Fig. 4).

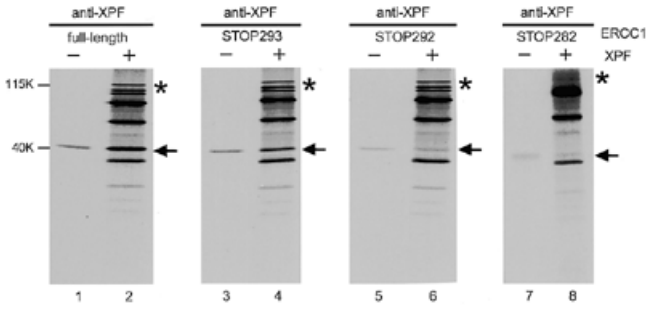

Figure 3. C-Terminal truncations of ERCC1. Autoradiogram of (antibody bead-bound) ^{35}S-labeled proteins separated on an 11% SDS–polyacrylamide gel. Arrows indicate (truncated) ERCC1 products, asterisks indicate full-length XPF. The odd lanes show non-specific binding of ERCC1 fragments to anti-XPF antibody beads. Interaction with XPF is scored positive if the amount of precipitated ERCC1 is significantly more in the presence (even lanes) than in the absence (odd lanes) of XPF. In each precipitation (lanes 1–8), similar amounts of ERCC1 products were used. Note that ERCC1-STOP293 specifically binds to XPF, but with reduced affinity compared with full-length ERCC1 (compare lanes 4 and 2). The molecular weights of the proteins are indicated.

The ERCC1-binding domain is localized to the C-terminal region of XPF

Figure 1 shows that a complete series of truncated XPF fragments originating from alternative translational start sites co-precipitate with wild-type ERCC1 when an anti-ERCC1 antibody is used (Fig. 1, lane 3). This indicates that the C-terminal part of XPF is responsible for ERCC1 binding, which would be in agreement with the Rad10-binding domain in Rad1, which was mapped to

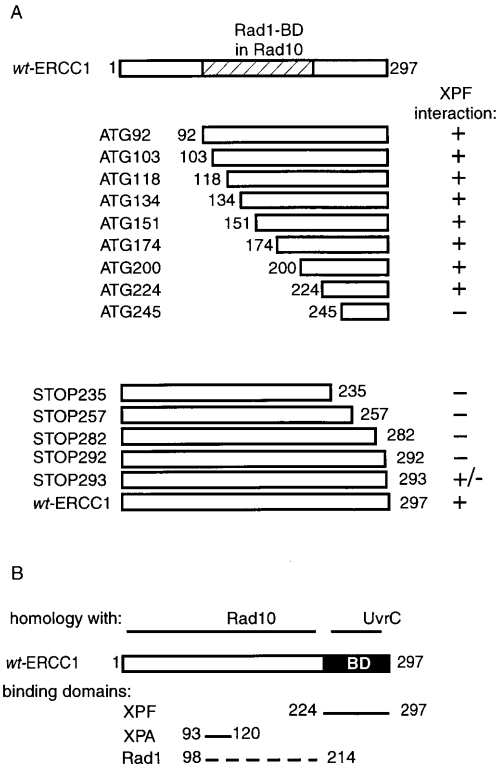

Figure 4. Schematic presentation of the XPF-binding domain in ERCC1. (**A**) Overview of XPF interactions obtained with truncated ERCC1 fragments. At the top is shown full-length ERCC1 with the domain that corresponds to the Rad1-binding domain (BD) in Rad10. +, interaction with XPF; +/–, intermediate interaction with XPF; –, no specific interaction with XPF. (**B**) Mapping of the XPF-binding domain (BD) in ERCC1. (Below) A summary of reported interaction domains in ERCC1. The dotted line represents Rad1–Rad10 BD; note that Rad1 and ERCC1 do not physically interact (Discussion).

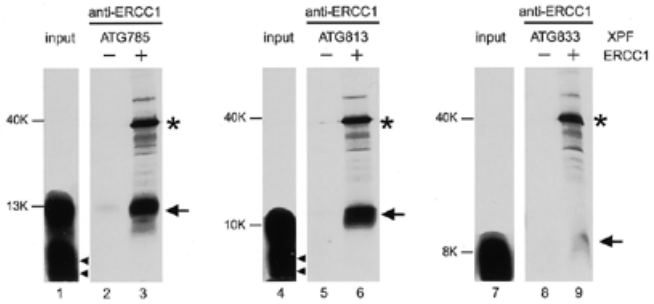

Figure 5. N-Terminal truncations of XPF. Autoradiogram of (antibody bead-bound) ^{35}S-labeled proteins separated on a 15% SDS–polyacrylamide gel. Arrows indicate truncated XPF product, asterisks indicate full-length ERCC1 protein and arrowheads (lanes 1 and 4) indicate XPF products originating from the alternative starts at position 844 and 856. Note that these two truncated XPF fragments do not co-precipitate with ERCC1 (lanes 3 and 6), confirming the mapping of the N-terminal border of the ERCC1-binding domain in XPF. Lanes 2, 5 and 8 show non-specific binding of XPF fragments to anti-ERCC1 antibody beads. Input is shown in this figure to demonstrate that although some XPF-ATG833 specifically co-precipitates with ERCC1 (compare lanes 9 and 8), the ERCC1 affinity of this XPF fragment is strongly reduced (compare lanes 9 and 7 with lanes 6 and 4 and 3 and 1). The molecular weights of the proteins are indicated.

a region corresponding to residuess 662–827 in XPF (37). To identify the ERCC1-interacting region in the XPF protein, initially a set of N-terminally truncated XPF cDNAs was made by systematically removing coding DNA on the 5′-side of in-frame ATG codons. In this way we obtained the constructs XPF-ATG629, XPF-ATG677, XPF-ATG711 and XPF-ATG737. On polyacrylamide gels, the *in vitro* translated products of these constructs co-migrated exactly with the truncated fragments that were synthesized along with full-length XPF. Precipitation studies with full-length ERCC1 showed that not only XPF-ATG629, lacking the N-terminal 629 residues, but also the other N-terminally truncated XPF fragments were fully capable of binding ERCC1 (data not shown, but see below for further truncations). This demonstrated directly that, like Rad1, XPF contains a large N-terminal region that is dispensable for complex formation, but it also showed that the interaction domain in XPF is located more towards the C-terminus. By means of PCR, we further truncated the XPF protein and found that ERCC1 affinity was unaffected even when almost 90% of residues were missing from the N-terminus of the XPF protein; the peptides XPF-ATG758 (Fig. 6, lanes 1 and 2), XPF-ATG785 (Fig. 5, lanes 1–3) and XPF-ATG813 (Fig. 5, lanes 4–6) all bound strongly to the ERCC1 protein. However, ERCC1 binding capacity was severely reduced when 20 more residues were deleted from the N-terminus of XPF (XPF-ATG833; Fig. 5, lanes 7–9). Thus, the N-terminal border of the ERCC1 interaction domain is located between residues 814 and 834 in XPF.

To map the C-terminal border of the ERCC1-binding domain in XPF, premature translational stops at positions 845 and 875 were introduced into the binding-proficient XPF-ATG677 construct, reducing its length by 60 and 30 amino acids, respectively. This yielded the peptides XPF677–845 and XPF677–875. Unlike a (smaller) peptide that contained the very C-terminal residues of XPF (XPF758–905), neither XPF677–845 nor XPF677–875 showed specific binding to ERCC1 (Fig. 6), demonstrating that the C-terminal border of the ERCC1-binding domain in XPF resides between amino acids 875 and 905 (Fig. 7).

Direct interaction between the binding domains of ERCC1 and XPF

The minimal domain required for initial and stable XPF binding spans residues 224–297 in ERCC1, whereas residues 814–905 in XPF were found to be necessary and sufficient for stable binding to ERCC1. To find out whether these domains physically interact, we mixed the HA-tagged peptide ERCC1224–297 with XPF813–905 and precipitated them with an anti-HA antibody. Since these two peptides migrate similarly on SDS–polyacrylamide gels, radiolabeled methionines were only incorporated into XPF813–905. XPF813–905 was found to co-precipitate with ERCC1224–297 (Fig. 8, lane 2), but not with the smaller ERCC1245–297 fragment (Fig. 8, lane 3, compare with lane 1), demonstrating that ERCC1–XPF complex formation is established by a direct interaction between residues 224–297 of ERCC1 and 814–905 of XPF.

Naturally occurring XPF mutations affect complex formation

Mutational analysis of an XP-F patient, XP126LO (39), demonstrated sequence alterations in the C-terminal part of both XPF alleles, one being a point mutation resulting in an amino acid

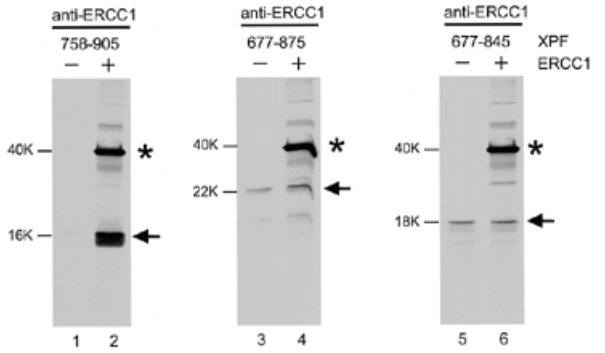

Figure 6. C-Terminal truncations of XPF. Autoradiogram of (antibody bead-bound) ^{35}S-labeled proteins separated on a 15% SDS–polyacrylamide gel. Arrows indicate XPF fragments, asterisks indicate full-length ERCC1 protein. Odd lanes show non-specific binding of XPF fragments to anti-ERCC1 antibody beads. Equal amounts of XPF products were used in each precipitation (lanes 1–6). Note that although XPF 677–875 (lanes 3 and 4) and XPF677–845 (lanes 5 and 6) are larger than XPF758–905 (lanes 1 and 2), they do not precipitate with ERCC1, due to C-terminal deletions. The molecular weights of the proteins are indicated.

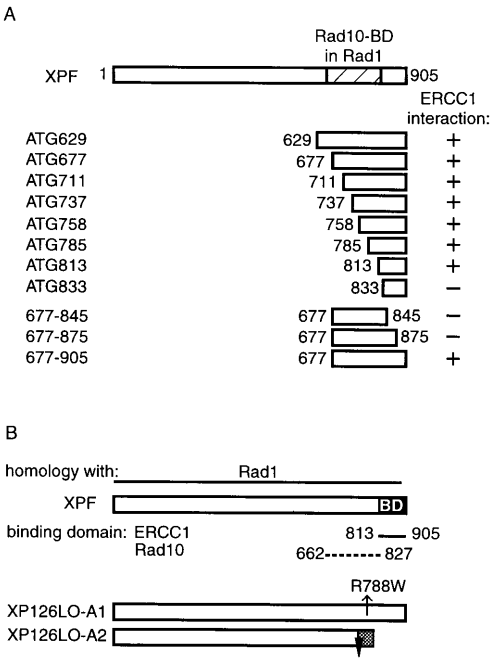

Figure 7. Schematic presentation of the ERCC1-binding domain in XPF. (**A**) Overview of ERCC1 interactions obtained with truncated XPF fragments. At the top is shown full-length XPF with the domain that corresponds to the Rad10-binding domain in Rad1. +, interaction with ERCC1; –, no specific interaction with ERCC1. (**B**) Mapping of the ERCC1-binding domain in XPF (BD) and schematic presentation of the XP126LO alleles. The arrow indicates the position of the R788W substitution in allele 1 of XP126LO. The triangle indicates the position of the frameshift resulting in a truncated protein in allele 2 of XP126LO.

change at position 788 (R788W) and the other being a 4 nt deletion causing a frameshift at residue 757 and a premature truncation at position 803. Strongly reduced protein levels of both ERCC1 and XPF were observed in cells of this patient, apparently as a consequence of these XPF mutations. Previous observations indicated that ERCC1 and XPF molecules residing outside the complex are rapidly degraded in the cell. We therefore hypothesized that these mutations would interfere with stable complex formation (14). To test this directly, cDNAs encoding the two XP126LO alleles were cloned into expression vectors and *in vitro* translated. Co-precipitations with wild-type ERCC1 translates revealed that the amino acid substitution R788W did not alter the ERCC1 binding capacity of XPF protein (Fig. 9, lane 3), whereas the product of the other allele had completely lost it (Fig. 9, lane 4). Thus, one of the alleles of this XP-F patient indeed carries a mutation that affects ERCC1 binding *in vitro*. However, under the conditions used here, no altered ERCC1 affinity was observed for the gene product carrying the point mutation at position 788.

DISCUSSION

In this study we mapped the interaction domains between two polypeptides by performing immunoprecipitations on *in vitro* translated proteins. In such assays, small amounts of both proteins are mixed in the context of a huge excess of unrelated, reticulocyte lysate-derived, proteins. Co-precipitation, therefore, requires that proteins bind each other with relatively high affinity. A well-established interaction between ERCC1 and XPA for example, with a dissociation constant of 2.5×10^{-7} M (40), cannot be visualized with this procedure and co-precipitation of *in vitro* translated XPA is only detected with an excess of (recombinantly overproduced) ERCC1 on antibody beads (41; unpublished observation). Thus, our binding assay is a conservative one that will only reveal domains required for initial and stable complex formation, but fails to show residue stretches of minor importance for protein–protein interactions. We define residues 224–297 in ERCC1 and 814–905 in XPF as the regions responsible for initial and stable complex formation between ERCC1 and XPF.

Comparison between ERCC1–XPF and Rad1–Rad10

Rad1–Rad10 from *S.cerevisiae* and mammalian ERCC1–XPF not only display extensive amino acid sequence homology, but are also functionally very similar. Both complexes interact with the DNA damage-binding NER protein XPA, which is known as Rad14 in *S.cerevisiae* (22,42,43). Also, both display identical incision patterns on stem–loop substrates (8) and require similar DNA structural elements for nuclease activity (6,44). Interaction domains responsible for complex formation have previously been assigned to the Rad1–Rad10 complex, using a two-hybrid system and immunoprecipitation assays similar to those described in this report (37,38). The binding domains in both Rad1 and Rad10 appeared to map to protein regions that are well conserved between the yeast and mammalian homologs. Suprisingly, however, we find that the interaction domains in ERCC1 and XPF locate elsewhere.

The location of the Rad1-binding domain in Rad10 corresponds to residues 98–214 in ERCC1 (37), but the XPF-binding domain in ERCC1 comprises a stretch of amino acids (224–297) that resides outside the region of homology with Rad10 (Fig. 4b). This C-terminal extension in ERCC1 is predominantly composed of a double HhH motif (residues 236–289). HhH motifs have been found in many DNA break processing enzymes, including the *E.coli* NER protein UvrC, and are thought to be involved in DNA binding. Previous mutagenesis studies showed that a ‘Rad10-like’ ERCC1 protein, with a stop at residue 214, was

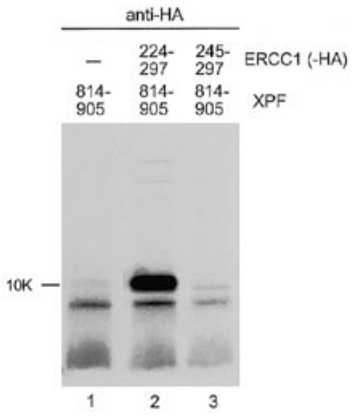

Figure 8. Direct interaction between the binding domains of ERCC1 and XPF. Only ERCC1 fragments contained an HA epitope tag at the C-terminus. Precipitations were performed with an anti-HA antibody. No radiolabel was incorporated into ERCC1 fragments. The molecular weight of XPF813–905 is indicated.

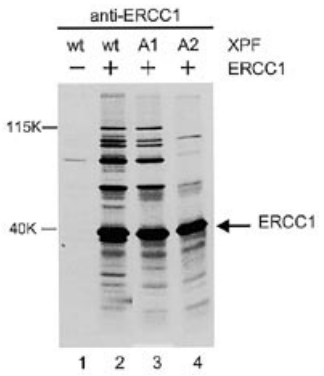

Figure 9. A naturally occurring XPF mutation affects complex formation with ERCC1. Autoradiogram of (antibody bead-bound) ^{35}S-labeled proteins separated on an 11% SDS–polyacrylamide gel. The arrow indicates ERCC1 protein. wt, wild-type XPF protein; A1, allele 1 of patient XP126LO carrying the R788W mutation; A2, allele 2 carrying the frameshift at position 757. Similar amounts of XPF were used in each precipitation (lanes 1–4). The molecular weights of the proteins are indicated.

functionally inactive (27). This can now be explained by the inability of this protein to form a complex with XPF. However, addition of a double HhH motif alone is not sufficient to restore XPF binding capacity. A hybrid protein containing the first 236 amino acids of ERCC1 fused to the double HhH motif of bacterial UvrC, composing a peptide of 291 amino acids, failed to bind XPF (data not shown). Similarly, the ERCC1-STOP292 peptide containing the complete double HhH motif of ERCC1 did not bind XPF (Fig. 3). Apparently, the double HhH motif in ERCC1 is not directly involved in XPF binding. Our data demonstrate that residues 293–297 in ERCC1 are important for XPF binding. Interestingly, an as yet unobserved homology exists between the C-terminal residues 293–296 in ERCC1, comprising the amino acids Phe-Leu-Lys-Val, and the final four residues of Rad10 (207–210), which are Tyr-Leu-Asn-Leu. Although the Rad1-binding motif in Rad10 was reported to extend to residue 210 (37), to our knowledge no subtle truncations from the C-terminus of Rad10 have been made. Hence, it is not clear whether these particular four residues of Rad10 are indispensable for Rad1 binding, but it is possible that the two motifs in ERCC1 and Rad10 fulfil similar roles in binding the complexing protein partner. Along this line of argument, the double HhH motif present in ERCC1 may support correct structural positioning of the very C-terminal residues of ERCC1. The functional relevance of an additional, putative DNA-binding domain in this part of ERCC1 still has to be resolved though. It is worth mentioning that *S.pombe* Swi10 (45) and plant homologs of ERCC1 (46) also contain a UvrC-like C-terminal domain, which suggests that *S.cerevisiae* Rad10 is an exception in lacking this region.

XPF and Rad1 use partially different domains for binding their respective complexing partners as well. The Rad10-binding domain in Rad1 has homology to residues 662–827 in XPF, but we find that residues 814–905 in XPF are required for actual ERCC1 binding. Motifs with a putative function have not been found in this region (8). The poorly conserved localization of interaction domains between *S.cerevisiae* Rad1–Rad10 and human ERCC1–XPF explains why neither *in vivo* nor *in vitro* was an interspecies protein–protein interaction observed between Rad1 and ERCC1 (37).

Interpretation of ERCC1 and XPF mutations

Recently, we reported a mutational analysis of the *ERCC1* gene in which a series of truncated ERCC1 proteins were tested for repair capacity *in vivo* (14). The N-terminal 92 amino acids were found to be dispensable for ERCC1 to function in repair *in vivo*. Disruption of the N-terminal 103 residues of ERCC1, however, completely destroyed the repair capacity of this peptide. As in our precipitation assay this protein fragment is capable of binding XPF, effects on ERCC1–XPF complex formation seem not to be involved. Rather, a reduced affinity for XPA, whose binding domain maps to residues 93–120 in ERCC1, may underly this phenotype. C-Terminal ERCC1 truncations demonstrated a direct link between complex formation ability and repair capacity. A deletion of five amino acids from the C-terminus of ERCC1 (ERCC1-STOP292) completely destroyed both the protein's ability to bind to XPF (Fig. 3) and to support repair *in vivo* (14). However, addition of only one residue to this peptide, Phe293 in ERCC1-STOP293, not only partially restored XPF binding (Fig. 3), but was also sufficient for partial restoration of the *in vivo* repair capacity of ERCC1 (14). Apparently, Phe293 in ERCC1 is crucial for XPF affinity and complex formation is a prerequisite for ERCC1 to function in repair.

Reduced protein levels, not only of XPF but also of ERCC1, are frequently observed in XP-F patients (48; personal observation). The instability of these proteins is thought to be caused by the lack of a stably bound partner. A similar phenomenon has been observed with other tight protein complexes, for example with Ku70/Ku80 (49). XP126LO is an XP-F patient with such reduced XPF and ERCC1 protein levels whose mutations have been mapped. One allele carries a frameshift at residue 757, which leads to a premature stop in front of the ERCC1-binding domain and, in agreement, we find that the encoded protein does not interact with ERCC1. The R788W point mutation in the other allele resides outside the ERCC1-binding region in XPF and we find that this mutated XPF protein binds normally to ERCC1. However, as residual XPF and ERCC1 protein levels in this patient are <50%, this mutation is also anticipated to affect

complex formation. Apparently, additional low affinity interaction domains not picked up in our conservative assay can still be of significant relevance for *in vivo* complex stability. Of course, the possibility that R788W makes XPF proteolytically unstable by itself cannot be dismissed here. Either way, the residual complexes observed in this patient must contain XPF molecules carrying the R788W substitution; this mutated form of XPF is responsible for the phenotypic features of the XP126LO patient, which is supported by our recent finding of a homozygous R788W defect in another XP-F patient with similar responses to UV (N.G.J.Jaspers, unpublished results). Residual ERCC1–XPF protein amounts are likely to be required for normal development and viability, since mice carrying a homozygous null mutation in *ERCC1* show developmental delay, severe liver and kidney abnormalities, reduced lifespan and signs of premature senescence (16,19). As most XP-F patients tested have reduced ERCC1 and XPF protein levels (48; unpublished observations), we expect that partially disrupted ERCC1 affinity frequently underlies the XP-F phenotype.

ACKNOWLEDGEMENT

This work was financially supported by the Dutch Scientific Organization (NWO, Foundation for Chemical Sciences).

REFERENCES

1 Huang,J.C., Svoboda,D.L., Reardon,J.T. and Sancar,A. (1992) *Proc. Natl Acad. Sci. USA*, **89**, 3664–3668.
2 Moggs,J.G., Yarema,K.J., Essigmann,J.M. and Wood,R.D. (1996) *J. Biol. Chem.*, **271**, 7177–7186.
3 Mu,D., Park,C.-H., Matsunaga,T., Hsu,D.S., Reardon,J.T. and Sancar,A. (1995) *J. Biol. Chem.*, **270**, 2415–2418.
4 Aboussekhra,A., Biggerstaff,M., Shivji,M.K.K., Vilpo,J.A., Moncollin,V., Podust,V.N., Protic,M., Hubscher,U., Egly,J.-M. and Wood,R.D. (1995) *Cell*, **80**, 859–868.
5 Friedberg,E.C., Walker,G.C. and Siede,W. (1995) *DNA Repair and Mutagenesis*. ASM Press, Washington, DC.
6 de Laat,W.L., Appeldoorn,E., Jaspers,N.G.J. and Hoeijmakers,J.H.J. (1998) *J. Biol. Chem.*, **273**, 7835–7842.
7 Matsunaga,T., Mu,D., Park,C.-H., Reardon,J.T. and Sancar,A. (1995) *J. Biol. Chem.*, **270**, 20862–20869.
8 Sijbers,A.M., de Laat,W.L., Ariza,R.R., Biggerstaff,M., Wei,Y.-F., Moggs,J.G., Carter,K.C., Shell,B.K., Evans,E., de Jong,M.C., Rademakers,S., de Rooij,J., Jaspers,N.G.J., Hoeijmakers,J.H.J. and Wood,R.D. (1996) *Cell*, **86**, 811–822.
9 O'Donovan,A., Davies,A.A., Moggs,J.G., West,S.C. and Wood,R.D. (1994) *Nature*, **371**, 432–435.
10 Evans,E., Fellows,J., Coffer,A. and Wood,R.D. (1997) *EMBO J.*, **16**, 625–638.
11 Evans,E., Moggs,J., Hwang,J., Egly,J.-M. and Wood,R.D. (1997) *EMBO J.*, **16**, 6559–6573.
12 Mu,D., Wakasugi,M., Hsu,D. and Sancar,A. (1997) *J. Biol. Chem.*, **272**, 28971–28979.
13 Busch,D., Greiner,C., Lewis,K., Ford,R., Adair,G. and Thompson,L. (1989) *Mutagenesis*, **4**, 349–354.
14 Sijbers,A.M., van der Spek,P.J., Odijk,H., van den Berg,J., van Duin,M., Westerveld,A., Jaspers,N.G.J., Bootsma,D. and Hoeijmakers,J.H.J. (1996) *Nucleic Acids Res.*, **24**, 3370–3380.
15 De Vries,A., van Oostrom,C.T.M., Hofhuis,F.M.A., Dortant,P.M., Berg,R.J.W., de Gruijl,F.R., Wester,P.W., van Kreijl,C.F., Capel,P.J.A., van Steeg,H. and Verbeek,S.J. (1995) *Nature*, **377**, 169–173.
16 McWhir,J., Seldridge,J., Harrison,D.J., Squires,S. and Melton,D.W. (1993) *Nature Genet.*, **5**, 217–223.
17 Nakane,H., Takeuchi,S., Yuba,S., Saijo,M., Nakatsu,Y., Ishikawa,T., Hirota,S., Kitamura,Y., Kato,Y., Tsunoda,Y., Miyauchi,H., Horio,T., Tokunaga,T., Matsunaga,T., Nikaido,O., Nishimune,Y., Okada,Y. and Tanaka,K. (1995) *Nature*, **377**, 165–168.
18 Sands,A.T., Abuin,A., Sanchez,A., Conti,C.J. and Bradley,A. (1995) *Nature*, **377**, 162–165.
19 Weeda,G.D., Donker,I., de Wit,J., Morreau,H., Janssens,R., Vissers,C.J., Nigg,A., van Steeg,H., Bootsma,D. and Hoeijmakers,J.H.J. (1997) *Curr. Biol.*, **7**, 427–439.
20 Fishman-Lobell,J. and Haber,J.E. (1992) *Science*, **258**, 480–484.
21 Gutz,H. and Schmidt,H. (1985) *Curr. Genet.*, **9**, 325–331.
22 Li,L., Elledge,S.J., Peterson,C.A., Bales,E.S. and Legerski,R.J. (1994) *Proc. Natl Acad. Sci. USA*, **91**, 5012–5016.
23 Park,C.-H., Bessho,T., Matsunaga,T. and Sancar,A. (1995) *J. Biol. Chem.*, **270**, 22657–22660.
24 Robins,P., Jones,C.J., Biggerstaff,M., Lindahl,T. and Wood,R.D. (1991) *EMBO J.*, **10**, 3913–3921.
25 Bessho,T., Sancar,A., Thompson,L.H. and Thelen,M.P. (1997) *J. Biol. Chem.*, **272**, 3833–3837.
26 Matsunaga,T., Park,C.-H., Bessho,T., Mu,D. and Sancar,A. (1996) *J. Biol. Chem.*, **271**, 11047–11050.
27 van Duin,M., van den Tol,J., Warmerdam,P., Odijk,H., Meijer,D., Westerveld,A., Bootsma,D. and Hoeijmakers,J.H.J. (1988) *Nucleic Acids Res.*, **16**, 5305–5322.
28 Doolittle,R.F., Johnson,M.S., Husain,I., Van Houten,B., Thomas,D.C. and Sancar,A. (1986) *Nature*, **323**, 451–453.
29 Lin,J.J. and Sancar,A. (1991) *Proc. Natl Acad. Sci. USA*, **88**, 6824–6828.
30 Moolenaar,G., Uiterkamp,R., Zwijnenburg,D. and Goosen,N. (1998) *Nucleic Acids Res.*, **26**, 462–468.
31 Doherty,A.S., Serpell,L.C. and Ponting,C.P. (1996) *Nucleic Acids Res.*, **24**, 2488–2497.
32 Harrington,J.J. and Lieber,M.R. (1994) *EMBO J.*, **13**, 1235–1246.
33 Lieber,M.R. (1997) *BioEssays*, **19**, 233–240.
34 van Vuuren,A.J., Appeldoorn,E., Odijk,H., Yasui,A., Jaspers,N.G.J., Bootsma,D. and Hoeijmakers,J.H.J. (1993) *EMBO J.*, **12**, 3693–3701.
35 Christy,K.J., LaTart,D. and Osterhoudt,W. (1989) *BioTechniques*, **7**, 692–693.
36 Biggerstaff,M., Szymkowski,D.E. and Wood,R.D. (1993) *EMBO J.*, **12**, 3685–3692.
37 Bardwell,A.J., Bardwell,L., Johnson,D.K. and Friedberg,E.C. (1993) *Mol. Microbiol.*, **8**, 1177–1188.
38 Bardwell,L., Cooper,A.J. and Friedberg,E.C. (1992) *Mol. Cell. Biol.*, **12**, 3041–3049.
39 Norris,P.G., Hawk,J.L.M. and Giannelli,F. (1988) *J. Am. Acad. Dermatol.*, **18**, 1185–1188.
40 Saijo,M., Kuraoka,I., Masutani,C., Hanaoka,F. and Tanaka,K. (1996) *Nucleic Acids Res.*, **24**, 4719–4724.
41 Bessho,T., Mu,D. and Sancar,A. (1997) *Mol. Cell. Biol.*, **17**, 6822–6830.
42 Guzder,S., Sung,P., Prakash,L. and Prakash,S. (1996) *J. Biol. Chem.*, **271**, 8903–8910.
43 Park,C.-H. and Sancar,A. (1994) *Proc. Natl Acad. Sci. USA*, **91**, 5017–5021.
44 Bardwell,A.J., Bardwell,L., Tomkinson,A.E. and Friedberg,E.C. (1994) *Science*, **265**, 2082–2085.
45 Rodel,C., Kirchhoff,S. and Schmidt,H. (1992) *Nucleic Acids Res.*, **20**, 6347–6353.
46 Xu,H., Swoboda,I., Bhalla,P.L., Sijbers,A.M., Zhao,C., Ong,E.-K., Hoeijmakers,J.H.J. and Singh,M.B. (1998) *Plant J.*, **13**, 823–829.
47 Yagi,T., Wood,R.D. and Takebe,H. (1997) *Mutagenesis*, **12**, 41–44.
48 Chen,F., Peterson,S., Story,M. and Chen,D. (1996) *Mutat. Res.*, **362**, 9–19.
49 Satoh,M., Wang,J. and Reeves,W.H. (1995) *Eur. J. Cell. Biol.*, **66**, 127–135.